Excitation of multiple dipole surface plasmon resonances in spherical silver nanoparticles

Bjoern Niesen,[1,2*] Barry P. Rand,[1] Pol Van Dorpe,[1,2] Honghui Shen,[3] Bjorn Maes,[3] Jan Genoe,[1] and Paul Heremans[1,2]

[1]*imec vzw, Kapeldreef 75, B-3001 Leuven, Belgium*
[2]*Department of Electrical Engineering (ESAT), Katholieke Universiteit Leuven, Kasteelpark Arenberg 10, B-3001 Leuven, Belgium*
[3]*Department of Information Technology (INTEC), Ghent University-imec, St.-Pietersnieuwstraat 41, B-9000 Gent, Belgium*
**bjoern.niesen@imec.be*

Abstract: We observe the appearance of multiple dipole surface plasmon resonances in spherical Ag nanoparticles when embedded in an organic semiconductor that exhibits a highly dispersive permittivity. Comparing the absorption spectra of thin-films with and without Ag nanoparticles reveals the presence of two plasmon peaks. Numerical simulations and calculations based on an electrostatic model allow us to attribute both peaks to dipole resonances, and show that the strong dispersion of the organic permittivity is responsible for this behavior. The presence of these two plasmon resonances was found to enhance the absorption of the organic semiconductor over a broad wavelength range.

OCIS codes: (160.4236) Nanomaterials; (160.4890) Organic materials; (240.6680) Surface plasmons; (310.6860) Thin films, optical properties; (350.4990) Particles.

References and links

1. C. Noguez, "Surface plasmons on metal nanoparticles: the influence of shape and physical environment," J. Phys. Chem. C **111**(10), 3806–3819 (2007).
2. K. L. Kelly, E. Coronado, L. L. Zhao, and G. C. Schatz, "The optical properties of metal nanoparticles: the influence of size, shape, and dielectric environment," J. Phys. Chem. B **107**(3), 668–677 (2003).
3. D. D. Evanoff, Jr., R. L. White, and G. Chumanov, "Measuring the distance dependence of the local electromagnetic field from silver nanoparticles," J. Phys. Chem. B **108**(5), 1522–1524 (2004).
4. P. K. Jain, K. S. Lee, I. H. El-Sayed, and M. A. El-Sayed, "Calculated absorption and scattering properties of gold nanoparticles of different size, shape, and composition: applications in biological imaging and biomedicine," J. Phys. Chem. B **110**(14), 7238–7248 (2006).
5. J. J. Mock, D. R. Smith, and S. Schultz, "Local refractive index dependence of plasmon resonance spectra from individual nanoparticles," Nano Lett. **3**(4), 485–491 (2003).
6. J. N. Anker, W. P. Hall, O. Lyandres, N. C. Shah, J. Zhao, and R. P. Van Duyne, "Biosensing with plasmonic nanosensors," Nat. Mater. **7**(6), 442–453 (2008).
7. M.-C. Daniel, and D. Astruc, "Gold nanoparticles: assembly, supramolecular chemistry, quantum-size-related properties, and applications toward biology, catalysis, and nanotechnology," Chem. Rev. **104**(1), 293–346 (2004).
8. H. Haick, "Chemical sensors based on molecularly modified metallic nanoparticles," J. Phys. D Appl. Phys. **40**(23), 7173–7186 (2007).
9. H. A. Atwater, and A. Polman, "Plasmonics for improved photovoltaic devices," Nat. Mater. **9**(3), 205–213 (2010).
10. F. Hallermann, C. Rockstuhl, S. Fahr, G. Seifert, S. Wackerow, H. Graener, G. Plessen, and F. Lederer, "On the use of localized plasmon polaritons in solar cells," Phys. Status Solidi A **205**(12), 2844–2861 (2008).
11. B. P. Rand, P. Peumans, and S. R. Forrest, "Long-range absorption enhancement in organic tandem thin-film solar cells containing silver nanoclusters," J. Appl. Phys. **96**(12), 7519–7526 (2004).
12. A. J. Morfa, K. L. Rowlen, T. H. Reilly, M. J. Romero, and J. van de Lagemaat, "Plasmon-enhanced solar energy conversion in organic bulk heterojunction photovoltaics," Appl. Phys. Lett. **92**(1), 013504 (2008).
13. H. Shen, P. Bienstman, and B. Maes, "Plasmonic absorption enhancement in organic solar cells with thin active layers," J. Appl. Phys. **106**(7), 073109 (2009).
14. S. A. Choulis, M. K. Mathai, and V.-E. Choong, "Influence of metallic nanoparticles on the performance of organic electrophosphorescence devices," Appl. Phys. Lett. **88**(21), 213503 (2006).
15. M.-K. Kwon, J.-Y. Kim, B.-H. Kim, I.-K. Park, C.-Y. Cho, C. C. Byeon, and S.-J. Park, "Surface-plasmon-enhanced light-emitting diodes," Adv. Mater. **20**(7), 1253–1257 (2008).

#129207 - $15.00 USD Received 28 May 2010; revised 14 Jul 2010; accepted 11 Aug 2010; published 23 Aug 2010

16. S. Schlücker, "SERS microscopy: nanoparticle probes and biomedical applications," ChemPhysChem **10**(9-10), 1344–1354 (2009).
17. X. X. Han, B. Zhao, and Y. Ozaki, "Surface-enhanced Raman scattering for protein detection," Anal. Bioanal. Chem. **394**(7), 1719–1727 (2009).
18. U. Kreibig, and M. Vollmer, *Optical properties of metal clusters*, Springer Series in Materials Science (Springer-Verlag, 1995).
19. C. F. Bohren, and D. R. Huffman, *Absorption and scattering of light by small particles* (Wiley-Interscience, 1983).
20. K. L. Mutolo, E. I. Mayo, B. P. Rand, S. R. Forrest, and M. E. Thompson, "Enhanced open-circuit voltage in subphthalocyanine/C60 organic photovoltaic cells," J. Am. Chem. Soc. **128**(25), 8108–8109 (2006).
21. H. H. P. Gommans, D. Cheyns, T. Aernouts, C. Girotto, J. Poortmans, and P. Heremans, "Electro-optical study of subphthalocyanine in a bilayer organic solar cell," Adv. Funct. Mater. **17**(15), 2653–2658 (2007).
22. N. T. Fofang, T.-H. Park, O. Neumann, N. A. Mirin, P. Nordlander, and N. J. Halas, "Plexcitonic nanoparticles: plasmon-exciton coupling in nanoshell-J-aggregate complexes," Nano Lett. **8**(10), 3481–3487 (2008).
23. A A. J. Haes, S. Zou, J. Zhao, G. C. Schatz, and R. P. Van Duyne, "Localized surface plasmon resonance spectroscopy near molecular resonances," J. Am. Chem. Soc. **128**(33), 10905–10914 (2006).
24. G. Gupta, D. Tanaka, Y. Ito, D. Shibata, M. Shimojo, K. Furuya, K. Mitsui, and K. Kajikawa, "Absorption spectroscopy of gold nanoisland films: optical and structural characterization," Nanotechnology **20**(2), 025703 (2009).
25. P. Royer, J. L. Bijeon, J. P. Goudonnet, T. Inagaki, and E. T. Arakawa, "Optical absorbance of silver oblate particles - Substrate and shape effects," Surf. Sci. **217**(1-2), 384–402 (1989).
26. U. Kreibig, B. Schmitz, and H. D. Breuer, "Separation of plasmon-polariton modes of small metal particles," Phys. Rev. B Condens. Matter **36**(9), 5027–5030 (1987).
27. K. Tanabe, "Field enhancement around metal nanoparticles and nanoshells: a systematic investigation," J. Phys. Chem. C **112**(40), 15721–15728 (2008).
28. J. B. Khurgin, and G. Sun, "Enhancement of optical properties of nanoscaled objects by metal nanoparticles," J. Opt. Soc. Am. B **26**(12), B83–B95 (2009).
29. N. I. Cade, T. Ritman-Meer, and D. Richards, "Strong coupling of localized plasmons and molecular excitons in nanostructured silver films," Phys. Rev. B **79**(24), 241404 (2009).
30. T. K. Sau, A. L. Rogach, F. Jäckel, T. A. Klar, and J. Feldmann, "Properties and applications of colloidal nonspherical noble metal nanoparticles," Adv. Mater. **22**(16), 1805–1825 (2010).
31. B. P. Rand, J. Genoe, P. Heremans, and J. Poortmans, "Solar cells utilizing small molecular weight organic semiconductors," Prog. Photovolt. Res. Appl. **15**(8), 659–676 (2007).
32. B. C. Thompson, and J. M. J. Fréchet, "Polymer-fullerene composite solar cells," Angew. Chem. Int. Ed. Engl. **47**(1), 58–77 (2008).

1. Introduction

Metal nanoparticles (NPs) possess unique optical properties that arise from the collective oscillations of their free electrons when they are excited by an electromagnetic wave. The strength and frequency of this so-called localized surface plasmon resonance (LSPR) does not only depend on the metal NP size and shape, but is also highly sensitive to changes in the dielectric environment [1–5]. These properties give metal NPs potential applications in sensors [6–8], photovoltaic cells [9–13], light emitting devices [14,15], and surface-enhanced Raman scattering spectroscopy [16,17].

When a spherical metal NP is irradiated with light of a wavelength much larger than the particle radius R, it can be assumed that the NP is exposed to a spatially constant electromagnetic field and therefore only dipole LSPRs are excited [18,19]. According to this quasi-static approximation, the NP can be described as an ideal dipole with polarizability $\alpha(\omega)$ given by

$$\alpha(\omega) = 4\pi\varepsilon_0 R^3 \frac{\varepsilon_{\mathrm{NP}}(\omega) - \varepsilon_{\mathrm{m}}(\omega)}{\varepsilon_{\mathrm{NP}}(\omega) + 2\varepsilon_{\mathrm{m}}(\omega)}, \tag{1}$$

where ε_0 is the vacuum permittivity and ω the frequency of the incident electromagnetic wave, and $\varepsilon_{\mathrm{NP}}(\omega)$ and $\varepsilon_{\mathrm{m}}(\omega)$ denote the relative permittivity of the metal NP and the embedding medium, respectively. In general, both relative permittivities are complex numbers with $\varepsilon(\omega) = \varepsilon_1(\omega) + i\varepsilon_2(\omega)$. From Eq. (1), it follows that $\alpha(\omega)$ exhibits resonance behavior whenever $\left|\varepsilon_{\mathrm{NP}}(\omega) + 2\varepsilon_{\mathrm{m}}(\omega)\right|$ reaches a minimum. For a spherical metal NP in most embedding media, this dipole resonance condition is typically fulfilled once, either in the ultraviolet, visible or near-infrared wavelength range.

#129207 - $15.00 USD Received 28 May 2010; revised 14 Jul 2010; accepted 11 Aug 2010; published 23 Aug 2010

Here, however, we show that for spherical metal NPs in highly dispersive media, multiple dipole LSPRs can occur. As a highly dispersive medium we chose chloro[subphthalocyaninato]boron(III) (SubPc), an organic semiconducting molecule with very strong absorption in limited absorption bands and applications in organic solar cells [20,21]. The scientific literature offers multiple examples of studies of plasmonic systems embedded in highly dispersive media [22,23]. The uniqueness of the system studied here comes from the satisfaction of the dipolar resonance condition by the resonant behavior of the absorption bands of SubPc. We compare the light absorption of thin-films consisting of Ag NPs embedded in SubPc with that of pure SubPc thin-films, revealing not one, but two absorption bands due to the Ag NPs. By considering the relative permittivities of Ag and SubPc as well as numerical simulations that show good agreement with our experimental results, we are able to attribute the absorption in the Ag NPs at both bands to dipole LSPRs.

2. Experiments

Thin-films were deposited on glass (Corning Eagle XG) or Si/SiO_2 substrates by thermal evaporation at a chamber pressure below 2×10^{-6} Torr. A quartz-crystal oscillator was used to monitor the growth rate and layer thickness. The substrates were rotated during deposition, leading to a thickness inhomogeneity of < 5% over an area of 100 cm^2, as determined by spectroscopic ellipsometry. Using a computer-controlled retractable shadow mask, thin-films with up to six different thicknesses could be obtained in a single deposition run. Prior to deposition, the substrates were solvent cleaned followed by an ultraviolet/O_3 treatment for 15 min. Silver NPs were obtained by depositing Ag (99.99% purity, Kurt. J. Lesker Company) at 0.01 nm/s to a thickness of 1 nm, as determined by the quartz-crystal oscillator. SubPc (purchased from Sigma-Aldrich) was purified twice by thermal gradient sublimation and deposited at 0.1 nm/s either directly on the substrate or on top of the Ag NP layer.

The direct light transmission of thin-films on glass was measured using a Shimadzu UV-1601PC spectrophotometer, whereas the diffuse transmission and reflectance were measured using a Bentham PVE 300 photovoltaic device characterization system. As light scattering by the thin-films was found to be negligible, the light absorption was defined as absorption = 1 - direct transmission - reflectance. The absorption of the glass substrate was subtracted from all absorption spectra. The absorption differences between thin-films containing Ag NPs covered by SubPc and pure SubPc layers were obtained from samples that were coated in the same deposition run to ensure a minimal thickness variation. From six thin-films with the same nominal SubPc thickness deposited during a single run, the accuracy of the absorption difference spectra was estimated as ± 0.5% at wavelengths of $\lambda > 350$ nm. The uncertainty increased to ± 2% at $\lambda < 350$ nm due to the strong absorption of the glass substrate at these wavelengths. Relative permittivities of SubPc and Ag were determined from thin-films on Si/SiO_2 substrates using a SOPRA GESP-5 spectroscopic ellipsometer. The morphology of Ag NPs was determined by scanning electron microscopy (Hitachi SU8000) and atomic force microscopy in tapping mode (Veeco Dimension 3100 system with Nanoscope IV controller).

3. Results and discussion

A dense layer of Ag NPs, as observed from the scanning electron micrograph in Fig. 1(a), was obtained by depositing 1 nm of Ag by means of thermal evaporation. From above, the NPs possess a circular shape, with an average particle diameter of 7 nm and an inter-particle spacing comparable to the particle size. From atomic force microscopy measurements [Fig. 1(b)], an average NP height of 5 nm was determined. The absorption spectrum of the uncovered Ag NP layer is shown in Fig. 2(a) as a dashed curve and features a single band centered at $\lambda = 430$ nm. The small size of the Ag NPs compared to this wavelength allows us to apply the quasi-static approximation to determine whether a dipole LSPR is expected at this spectral position. Indeed, from Eq. (1), a single resonance at $\lambda = 360$ nm is obtained for a spherical Ag NP in vacuum [dashed curve in Fig. 2(f)], using the relative permittivity of Ag shown in Fig. 2(d). The absorption band can therefore be attributed to a dipole LSPR, red-shifted from the calculated value due to the presence of the substrate, interactions between the

#129207 - $15.00 USD Received 28 May 2010; revised 14 Jul 2010; accepted 11 Aug 2010; published 23 Aug 2010

NPs, and the deviation of the NP shape from a perfect sphere [24,25]. The absence of any further absorption bands is expected for spherical Ag NPs of this size and indicates that no higher order LSPR modes are excited [26].

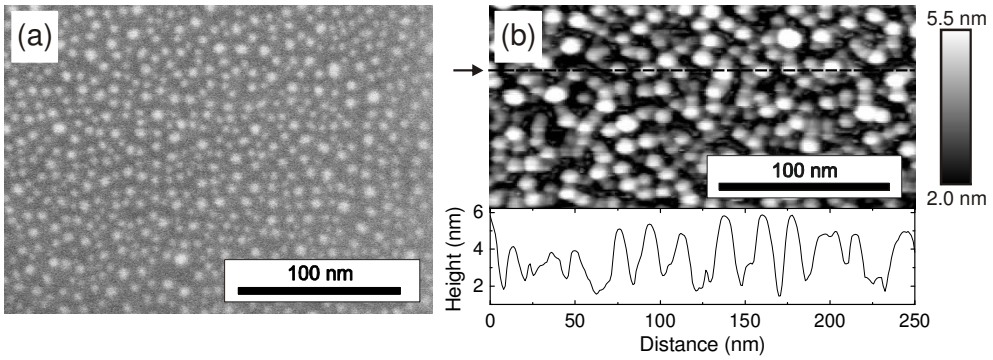

Fig. 1. (a) Scanning electron micrograph of Ag NPs obtained by depositing 1 nm of Ag on a Si/SiO_2 substrate by thermal evaporation. From above, the particles have a circular shape with an average diameter and inter-particle spacing of 7 nm. (b) Atomic force micrograph (top) of the Ag NPs on a glass substrate, with a height-profile (bottom) taken along the dashed line indicated by the arrow. An average NP height of 5 nm was determined from this micrograph. The lateral size of the NPs is overestimated due to convolution of the atomic force microscope tip and the sample features.

The absorption spectra of thin-films consisting of the Ag NP layer covered by 6 to 30 nm of SubPc are shown in Fig. 2(a) as solid curves, whereas the spectra of pure SubPc thin-films with the same thicknesses are shown in Fig. 2(b). In both cases, the strengths of the high energy Soret band (λ = 320 nm) and the low energy Q band (450 nm < λ < 630 nm) increase with increasing SubPc layer thickness. In order to determine the impact of the presence of the Ag NPs to the absorption of these layers, each absorption spectrum of the pure SubPc layers was subtracted from that of the thin-film consisting of Ag NPs and SubPc with the same layer thickness. These absorption differences feature two bands centered at λ = 445 nm and λ = 610-630 nm, as shown in Fig. 2(c). The intensity of both bands decreases with increasing SubPc thickness. It should be noted that for all SubPc layer thicknesses the peak wavelengths of the Soret and the Q bands are not altered by the presence of the Ag NPs. The low energy band observed in Fig. 2(c) rather results from an extension of the lowest energy absorption tail of the composite film shown in Fig. 2(a).

The analysis of this absorption difference is complicated by the fact that in addition to the absorption in the Ag NPs, contributions from enhanced absorption in the SubPc layer via the increased electromagnetic field surrounding the NPs are expected [27,28]. Such a plasmonic absorption enhancement has already been reported for Ag NPs embedded in the organic semiconductor copper phthalocyanine [11]. The wavelengths at which absorption in the Ag NPs contributes to the absorption difference can be estimated by applying Eq. (1) for a spherical Ag NP embedded in SubPc. The relative permittivity of SubPc is shown in Fig. 2(e). It is highly dispersive, with its real ($\varepsilon_{1,\mathrm{SubPc}}$) and imaginary part ($\varepsilon_{2,\mathrm{SubPc}}$) featuring an intense peak at λ = 603 nm and λ = 591 nm, respectively, corresponding to the strong light absorption of SubPc at these wavelengths. Interestingly, as a result of the highly dispersive permittivity of SubPc, two dipole LSPRs at λ = 430 and 624 nm are obtained from Eq. (1), as shown by the solid curve in Fig. 2(f). This agrees well with the observed absorption differences [open circles in Fig. 2(f)] and suggests that, indeed, dipole LSPRs contribute to both absorption bands.

In order to obtain further evidence for the nature of the absorption difference, numerical simulations were performed using COMSOL Multiphysics 3.5a. The geometry used for these three-dimensional simulations was motivated by our microscopy studies (Fig. 1) and is shown as an inset in Fig. 3(b). A periodic two-dimensional array of truncated Ag spheroids with a

#129207 - $15.00 USD Received 28 May 2010; revised 14 Jul 2010; accepted 11 Aug 2010; published 23 Aug 2010

height of 5 nm, a lateral dimension of 7 nm, and a center-to-center spacing of 14 nm represents the Ag NPs. The SubPc layers coating these truncated Ag spheroids have a thickness of either 10, 14, 18, 22 or 30 nm and a flat horizontal surface. As a reference, pure SubPc layers with the same thicknesses were simulated. The light is incident through the semi-infinite glass substrate ($\varepsilon_1 = 2.25$, $\varepsilon_2 = 0$), with the propagation vector **k** parallel to the y-axis and the electric field **E** parallel to the x-axis. The light absorption in the Ag and in SubPc was monitored separately. For the pure SubPc layers the monitored volume excluded the volume corresponding to the truncated Ag spheroids, such that the same SubPc volume was monitored for the layers with and without the Ag NPs.

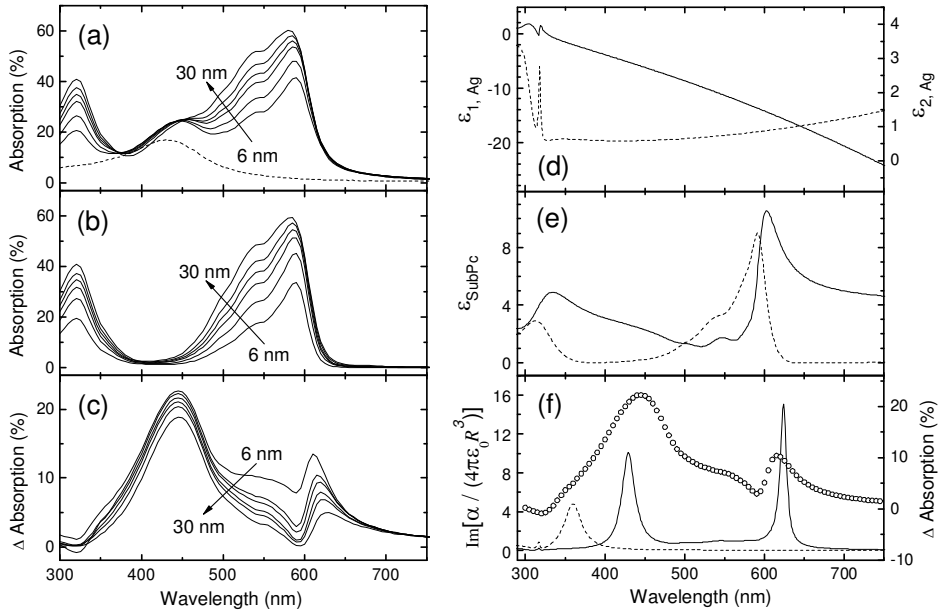

Fig. 2. (a) Absorption spectra of uncoated Ag NPs on glass (dashed curve) and Ag NPs covered by SubPc with a layer thickness of 6, 10, 14, 18, 22, and 30 nm (solid curves). (b) Absorption spectra of SubPc layers on glass, with the same thicknesses as in (a). (c) Difference between the absorption spectra of thin-films containing SubPc and Ag NPs shown in (a) and those of pure SubPc layers shown in (b) for each SubPc layer thickness. (d,e) Real (ε_1, solid curve) and imaginary part (ε_2, dashed curve) of the relative permittivity of (d) Ag and (e) SubPc. (f) The imaginary part of the dimensionless fraction of the polarizability, $\mathrm{Im}\left[\alpha / \left(4\pi\varepsilon_0 R^3\right)\right]$, for a spherical Ag NP in vacuum ($\varepsilon_m = 1$, dashed curve) and embedded in SubPc (solid curve). For comparison, the absorption difference between a thin-film consisting of the Ag NP layer covered by 10 nm of SubPc and a pure SubPc layer with a thickness of 10 nm is shown (open circles).

The difference between the absorption in the SubPc covering the truncated Ag spheroids and the pure SubPc layer is shown as a solid curve for each SubPc thickness in Fig. 3(a). These spectra show a broad band with two peaks at $\lambda = 452$ and 624 nm, and can be attributed to the plasmonic absorption enhancement in SubPc. The comparison with the simulated absorption spectra of a pure SubPc layer [dashed curve in Fig. 3(a)] reveals that this plasmonic absorption enhancement peaks at the blue and red absorption tail of the low energy Q band. The absorption in Ag for the truncated Ag spheroids covered by SubPc layers with different thicknesses is shown as solid curves in Fig. 3(b). These spectra feature two distinct bands centered at $\lambda = 446$ and 632 nm. For the absorption in the Ag as well as for the absorption difference in SubPc, the intensity of all bands decreases with increasing SubPc layer thickness.

#129207 - $15.00 USD Received 28 May 2010; revised 14 Jul 2010; accepted 11 Aug 2010; published 23 Aug 2010

The fact that the low energy peak in the simulated Ag absorption spectra is more intense than the high energy peak is in line with the resonance strengths obtained from Eq. (1) for a spherical Ag NP in SubPc. It is however in contrast to the experimentally observed absorption differences between SubPc thin-films with and without Ag NPs, which could be due to damping of the low energy LSPR by the inhomogeneous size and shape distribution of the Ag NPs. Qualitatively, however, these results are well in agreement with the experimentally observed results and clearly confirm the presence of absorption enhancement in SubPc at wavelengths above the high energy LSPR as well as the presence of two plasmon resonances in the Ag NPs surrounded by SubPc. Furthermore, as observed experimentally, the low energy resonance peak is not present in the case of the uncovered truncated Ag spheroids [dashed curve in Fig. 3(b)]. Finally, the x and y components of the electric field surrounding the truncated Ag spheroids covered by 10 nm of SubPc shown in Fig. 3(c) confirm that both LSPRs are indeed dipolar in nature.

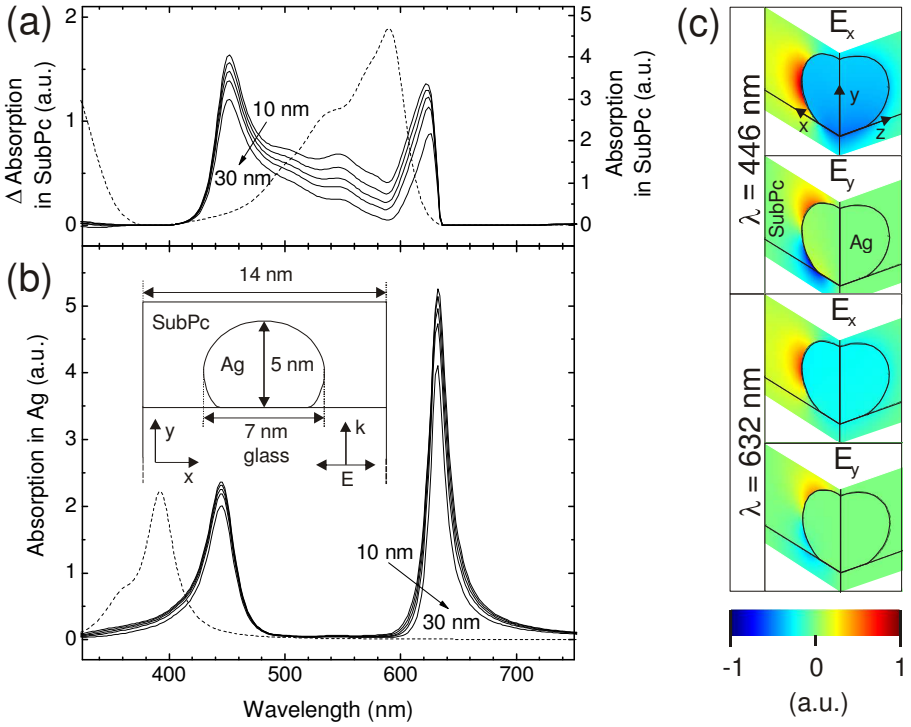

Fig. 3. Results of three-dimensional numerical simulations performed using a geometry with a cross-section as shown in the inset in (b). Periodic boundaries in both lateral dimensions result in an infinite two-dimensional array of truncated Ag spheroids with center-to-center spacing of 14 nm. The light wave is incident through the glass substrate with the propagation vector (**k**) and electric field vector **E** as indicated by arrows. (a) Difference between the absorption in the SubPc layers with thicknesses of 10, 14, 18, 22, and 30 nm covering the truncated Ag spheroids and the absorption in pure SubPc layers (excluding the volume corresponding to the truncated Ag spheroids) with the same thicknesses (solid curves). The absorption of a pure SubPc layer with a thickness of 10 nm is shown as a dashed curve. (b) Absorption in the uncovered truncated Ag spheroids (dashed curve) and in the truncated Ag spheroids covered by SubPc layers with the same thicknesses as in (a) (solid curves). (c) Surface plots of the x and y components of the electric field at λ = 446 and 632 nm for a SubPc thickness of 10 nm.

For similar metal NP-organic dye systems, the formation of hybridized exciton-plasmon polariton states caused by strong coupling has been reported, as evidenced by splitting of the absorption bands [22,29]. Indeed, both experimental results and simulations suggest the appearance of a weak shoulder at λ ~550 nm, which could be interpreted as the high energy hybrid state resulting from strong coupling between the low energy LSPR with the SubPc Q

#129207 - $15.00 USD Received 28 May 2010; revised 14 Jul 2010; accepted 11 Aug 2010; published 23 Aug 2010

band. In this strong coupling scenario, the Q band would therefore both provide the permittivity necessary to excite a dipolar resonance in the Ag nanoparticles, and at the same time strongly couple to this resonance to form hybrid states. However, further investigations are necessary to confirm the strong coupling scenario in this particular system.

4. Conclusions

In summary, we observed two bands from the absorption differences between thin-films consisting of a Ag NP layer covered by SubPc and pure SubPc thin-films. By means of numerical simulations, plasmonic absorption enhancement in the SubPc layer as well as absorption in the Ag NPs was found to contribute to both bands. By considering the simulated electric field surrounding the Ag NPs as well as calculations applying the quasi-static approximation, we were able to attribute the absorption in the Ag NPs at both absorption bands to dipole LSPRs. It should be further noted that the presence of multiple dipole resonances was not observed in the Ag NP layer without the SubPc medium surrounding it. Given this, we conclude that embedding spherical metal NPs in a highly dispersive medium can give rise to multiple absorption bands originating from dipole resonances, which is otherwise only exhibited by non-spherical NPs [30], and could be employed to broaden the spectral range of metal NP-based sensors. Furthermore, as the increase in absorption in SubPc benefits from the multiple LSPRs of the Ag NPs [Fig. 3(a)], this feature is expected to find application in organic solar cells, where enhanced absorption in the red tail of the absorption spectrum of the organic semiconductor should give rise to a corresponding increase in photocurrent [31,32].

Acknowledgments

The authors gratefully acknowledge Josine Loo for obtaining scanning electron micrographs, Alain Moussa for obtaining atomic force micrographs, and David Cheyns for measuring optical constants. This work was supported by the European Community's Seventh Framework Programme under Grant No. FP7-ICT-2009-4-248154 ("PRIMA"), the Institute for the Promotion of Innovation by Science and Technology in Flanders (IWT) via the SBO-project No. 060843 ("PolySpec"), the Belgian Interuniversity Attraction Poles program under Grant No. IAP P6-10 "photonics@be", and COST action MP 0702. P. Van Dorpe and B. Maes thank the Fonds Wetenschappelijk Onderzoek Vlaanderen (FWO)-Flanders for financial support.

#129207 - $15.00 USD Received 28 May 2010; revised 14 Jul 2010; accepted 11 Aug 2010; published 23 Aug 2010